Contribution from the Department of Chemistry,
University of Houston, Houston, Texas 77004

Electron-Transfer and Ligand-Addition Reactions of $(TPP)CrClO_4$ and (TPP)Cr(NO) in Nonaqueous Media[1]

S. L. KELLY and K. M. KADISH*

Received June 3, 1983

The electron-transfer and ligand-addition reactions of the chromium porphyrin complexes $(TPP)CrClO_4$ and (TPP)Cr(NO) were studied in 11 nonaqueous solvents. Studies of $(TPP)CrClO_4$ in noncoordinating solvents reveal a counterion dependence for the first reduction and first oxidation, suggesting metal-centered reactions. Spectrophotometric and electrochemical studies of $(TPP)CrClO_4$ in mixed-solvent systems provide clear evidence for the presence of the novel species $[(TPP)Cr(L)_2]^+$ in solution, where L = DMF, Me_2SO, and pyridine, and stepwise formation constants for the addition of pyridine and Me_2SO are determined. Conductometric studies combine with the mixed-solvent studies to suggest that the axial environment about the central metal determines the nature of the metal-centered reduction for (TPP)CrX. Electrochemical studies of (TPP)Cr(NO) show that nitrosylation stabilizes the divalent state by over 1.0 V, and metal-centered oxidation occurs via an EC mechanism. Studies in mixed-solvent systems provide formation constants for the addition of one coordinating base to (TPP)Cr(NO) and $[(TPP)Cr(NO)]^-$. Solvent dependences for the various redox reactions of $(TPP)CrClO_4$ and (TPP)Cr(NO) were correlated to solvent polarity scales and suggest that different solvent–solute interactions predominate for the two complexes.

Introduction

The reactions of chromium porphyrins have been the subject of several studies in the last 10 years[2-17] with special emphasis on measuring the interactions with oxygen[3-8] and diatomic ligands,[9,10] as well as determining the coordination number and related formation constants for axial ligation reactions with neutral donors.[11-16] These studies suggested that both chromium(II) and chromium(III) porphyrins can complex two axial ligands but that the symmetrical bisligated Cr(III) complex is not observed in solution. Spectrophotometric and conductometric studies on (TPP)CrCl by several workers[11,12,14] have shown that addition of a coordinating ligand produces (TPP)Cr(L)Cl readily in solution, but further ligand addition does not occur. Electrochemical studies on (TPP)CrCl by Bottomley and Kadish[15] have shown that formation of $[(TPP)Cr(py)_2]^+$ can be induced at the surface of an electrode by the application of potential, and a more complete electrochemical characterization of (TPP)CrCl has recently appeared.[16]

One objective of this paper is to report the spectrophotometric, conductometric, and electrochemical characterization of $(TPP)CrClO_4$, a complex in which axial interactions between the metal and counterion have been greatly reduced. These studies show conclusively that trivalent chromium porphyrin complexes can symmetrically coordinate two axial ligands and that displacement of counterion can occur. Furthermore, conductometric measurements and mixed-solvent studies show that the nature of axial coordination about the central metal plays the deciding role in determining the electrochemical reversibility of the metal-centered reduction. Another objective of this paper is to report the spectrophotometric and electrochemical characterization of the complex (TPP)Cr(NO). This continues our study on the interaction of metalloporphyrins with diatomic ligands,[18,19] which is pertinent toward understanding the role of metalloporphyrins in several important biological systems.

Experimental Section

Methods. Cyclic voltammetric experiments were made on either a PAR Model 174A polarographic analyzer or an IBM Model 225A voltammetric analyzer utilizing the three-electrode configuration of a Pt-button working electrode, a Pt-wire counterelectrode, and a commercially available saturated calomel electrode (SCE) as a reference electrode. An Omnigraphic 2000 X-Y recorder was used to record the current–voltage output. Half-wave potentials were measured as the average of the cathodic and anodic peak potentials, $(E_{p,a} + E_{p,c})/2$.

Coulometric experiments were performed with a PAR Model 173 potentiostat/galvanostat and Model 179 digital coulometer in conjunction with a Model 178 electrometer probe. A three-electrode configuration was used, consisting of a Pt-wire mesh working electrode, a Pt-wire counterelectrode separated from the main solution by a glass frit, and an SCE as the reference electrode. The coulometric cell contained a quartz window (2.0-mm path length) at the bottom, allowing the electronic absorption spectra of the reactant and product to be taken in situ. The configuration of the cell was such that bubbling of N_2 gas through the cell would allow all portions of the bulk solution to be reduced at the working electrode. A Tracor Northern 1710

(1) Abbreviations: TPP = 5,10,15,20-tetraphenylporphinato dianion; DN = Gutmann donor number; X = monovalent anion; L = ligand molecule; S = solvent molecule; β_n^m = formation constant for the addition of n ligand molecules to a metalloporphyrin complex with the metal in the m oxidation state; $MeCl_2$ = dichloromethane; $EtCl_2$ = 1,2-dichloroethane; PhCN = benzonitrile; MeCN = acetonitrile; n-PrCN = butyronitrile; THF = tetrahydrofuran; DMF = dimethylformamide; DMA = N,N-dimethylacetamide; Me_2SO = dimethyl sulfoxide; py = pyridine; TBAP = tetrabutylammonium perchlorate.

(2) Newton, C. W.; Davis, D. G. *J. Magn. Reson.* **1975**, *20*, 446–457.
(3) Groves, J. T.; Kruper, W. J., Jr.; Nemo, T. E.; Myers, R. S. *J. Mol. Catal.* **1980**, *7*, 169–177.
(4) Budge, J. R.; Gatehouse, B. M. K.; Nesbit, M. C.; West, B. O. *J. Chem. Soc., Chem. Commun.* **1981**, 370–371.
(5) Murakami, Y.; Matsuda, Y.; Yamada, S. *J. Chem. Soc., Dalton Trans.* **1981**, 855–861.
(6) Groves, J. T.; Kruper, W. J., Jr. *J. Am. Chem. Soc.* **1979**, *101*, 7613–7616.
(7) Buchler, J. W.; Kay, K. L.; Castle, L.; Ullrich, V. *Inorg. Chem.* **1982**, *21*, 842–844.
(8) Groves, J. T.; Kruper, W. J.; Haushalter, R. G.; Butler, W. M. *Inorg. Chem.* **1982**, *21*, 1363–1368.
(9) Cheung, S. K.; Grimes, C. J.; Wong, J.; Reed, C. A. *J. Am. Chem. Soc.* **1976**, *98*, 5028–5030.
(10) Wayland, B. B.; Olson, L. W.; Siddiqui, Z. U. *J. Am. Chem. Soc.* **1976**, *98*, 94–98.
(11) Summerville, D. A.; Jones, R. D.; Hoffman, B. M.; Basolo, F. J. *J. Am. Chem. Soc.* **1977**, *99*, 8195–8202.
(12) Basolo, F. J.; Jones, R. D.; Summerville, D. A. *Acta Chem. Scand., Ser. A* **1978**, *A32*, 771–780.
(13) Scheidt, W. R.; Brinegar, A. C.; Kirner, J. F.; Reed, C. A. *Inorg. Chem.* **1979**, *18*, 3610–3612.
(14) O'Brien, P.; Sweigart, D. A. *Inorg. Chem.* **1982**, *21*, 2094–2095.
(15) Bottomley, L. A.; Kadish, K. M. *J. Chem. Soc., Chem. Commun.* **1981**, 1212–1214.
(16) Bottomley, L. A.; Kadish, K. M. *Inorg. Chem.* **1983**, *22*, 342–349.
(17) Reed, C. A.; Kouba, J. K.; Grimes, C. J.; Cheung, S. K. *Inorg. Chem.* **1978**, *17*, 2666–2670.
(18) Olson, L. W.; Schaeper, D.; Kadish, K. M. *J. Am. Chem. Soc.* **1982**, *104*, 2042–2044.
(19) Lançon, D.; Kadish, K. M. *J. Am. Chem. Soc.* **1983**, *105*, 5610–5617.

0020-1669/84/1323-0679$01.50/0

holographic optical spectrometer/multichannel analyzer was used to obtain time-resolved spectra. Spectra result from the signal averaging of 100 sequential 5-ms spectral acquisitions. Each acquisition represents a single spectrum from 350 to 750 nm simultaneously recorded by a silicon diode array detector with a resolution of 1.2 nm/channel. Experiments at an optically transparent thin-layer electrode (OTTLE) were performed by using a cell specifically designed for nonaqueous solvents[20] in conjunction with the Tracor Northern 1710 optical spectrometer/multichannel analyzer.

For all electrochemical experiments, the reference electrode was separated from the bulk of solution by a fritted bridge filled with solvent and supporting electrolyte. The solution in the bridge was changed periodically to prevent aqueous contamination of the cell solution by the reference electrode. Deaeration of all solutions was accomplished by passing a constant stream of high-purity nitrogen or argon through the solution for 10 min and maintaining a blanket of inert gas over the solution during the experiment. The inert gas was saturated with solvent prior to entering the cell.

A Yellowstone International Model 31 conductivity bridge was used to measure solution conductances. Measurements were taken in a Fisher Scientific Co. Model 9-367 conductivity cell, which was immersed in a temperature bath with a controlled temperature of 25.00 ± 0.05 °C. The cell constant was determined by calibration to aqueous KCl solutions to be 0.545 cm^{-1}. All values are reported as molar conductances.

Infrared (IR) spectra were recorded on a Beckman Model 4250 infrared spectrophotometer. Samples were recorded as a Nujol mull between NaCl glass plates (Wilmad Glass Co.) or as KBr disks made in-house.

Calculation of Formation Constants from Spectrophotometric Data. Solutions for spectrophotometric measurements were prepared in $MeCl_2$ containing 0.1 M tetrabutylammonium perchlorate, TBAP, and metalloporphyrin. Aliquots of a $MeCl_2$ solution containing 0.1 M TBAP and coordinating base were added to this solution, and the absorbances were measured after each addition. The ligands reported are pyridine, Me_2SO, and DMF. Absorption spectra were obtained on a Cary 14 spectrophotometer at 25.00 ± 0.5 °C. For the case of (TPP)Cr(NO), the absorbance data could be fitted to the Hill equation,[32] and formation constants for the addition of one coordinating base were obtined by construction of Benesi–Hildebrandt plots (an example is shown in Figure 8). As the spectra obtained for (TPP)$CrClO_4$ were not simplified by the presence of isosbestic points over all ligand concentrations, the data were analyzed by SQUAD, a sophisticated computer program that tests various equilibrium models against a spectral data set and refines the initial estimates of stability constants for the model under consideration.[21,22] The application of SQUAD to the data allowed detection of mono and bis complexes of $[(TPP)Cr^{III}]^+$ for Me_2SO and pyridine and determination of the associated equilibrium constants. An application of SQUAD toward the determination of stability constants of metalloporphyrins has recently appeared.[23]

Materials. Tetrabutylammonium perchlorate, TBAP (Eastman), was twice recrystallized from ethanol and dried in vacuo at 40 °C prior to use. $(TPP)H_2$ was synthesized as per the method of Adler and co-workers[24] and was purified of any chlorin impurities by using the procedure of Barnett et al.[25] After recrystallization of the free base porphyrin from $MeCl_2$/MeOH solution, (TPP)CrCl was synthesized via the method of Summerville et al.[11] The crude product was chromatographed twice on basic alumina (Fisher Scientific) and was recrystallized from chloroform/hexane solutions. The purity of this material was verified by comparison of the visible spectra with literature spectra.[11] (TPP)$CrClO_4$ was the generous gift of Dr. Paul Minor and was synthesized by gently refluxing equimolar amounts of (TPP)CrCl and $AgClO_4$ (Alf Products) in THF solution. Filtration of the solution using a fine sintered-glass frit separated the resulting AgCl precipitate from the mother liquor. Evaporation of the THF left a dark green residue, which was recrystallized from toluene/hexane solution to give fine dark green crystals. The strategy employed to synthesize the perchlorate chromium complex parallels those published for the synthesis of the analogous perchlorate complexes of manganese[26] and iron[27] porphyrins. Comparison of the IR spectra of (TPP)$CrClO_4$ to that of (TPP)CrCl (Nujol mull) revealed new bands for (TPP)$CrClO_4$ at 1130 and 620 cm^{-1}, which is consistent with axially bound perchlorate. Further electronic absorption data for (TPP)$CrClO_4$ are presented in Table I. (TPP)Cr(NO) was synthesized from (TPP)CrCl via the method of Wayland and co-workers[10] using Schlenk Vacuum-line techniques. The purity of the nitrosyl complex was verified by comparison of the UV–visible, ESR, and IR absorbance spectra to those published for (TPP)Cr(NO).[10] Of interest is the presence in the Ir spectra of ν_{NO} at 1700 cm^{-1} (Nujol mull).

Table I. Absorbance Maxima (nm) of (TPP)$CrClO_4$ and (TPP)CrCl in Selected Solvents[a]

solvent	counterion	peak III	peak IV	peak V	peak VI
$MeCl_2$	ClO_4^-	604	566	452	400
	Cl^-	606	565	450	398
DMF	ClO_4^-	602	563	449	394
	Cl^-	605	565	447	395
Me_2SO	ClO_4^-	602	563	447	392
	Cl^-	608	568	449	394
py	ClO_4^-	607	570	458	406
	Cl^-	613	573	459	407

[a] Absorbance peaks are labeled according to ref 39. All solutions are 0.1 M in TBAP.

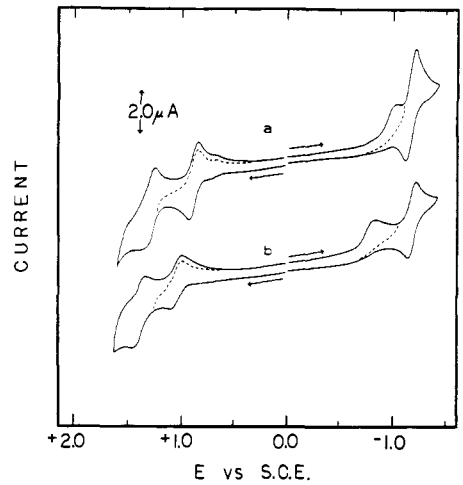

Figure 1. Cyclic voltammograms of (a) 1.3×10^{-3} M (TPP)CrCl and (b) 10^{-3} M (TPP)$CrClO_4$ dissolved in $MeCl_2$/0.1 M TBAP solutions (scan rate 0.20 V/s).

Eleven different nonaqueous, aprotic solvents were used throughout this study. Dimethyl sulfoxide, Me_2SO (Eastman Chemical), dimethylacetamide, DMA (Fisher Scientific), and benzonitrile, PhCN (Aldrich Chemical) were received as reagent grade from the manufacturer and were dried over 4-Å molecular sieves prior to use. Dichloroethane, $EtCl_2$, was purchased from Mallinckrodt. Prior to use, portions were extracted with equal volumes of concentrated H_2SO_4, distilled H_2O, and a 5% KOH solution. The extract was then distilled from P_2O_5 and stored in the dark over activated 4-Å molecular sieves. Methylene chloride, $MeCl_2$, obtained from Fisher Scientific as technical grade was treated in a similar fashion. Butyronitrile, *n*-PrCN, was obtained from Aldrich Chemical and was purified by the method of Van Duyne and Reilley.[28] Matheson Coleman and Bell was the supplier for acetonitrile, MeCN, and acetone, $(CH_3)_2CO$, which were dried over 4-Å molecular sieves after distillation. Tetrahydrofuran, THF, was also supplied by Matheson Coleman and Bell. This solvent was distilled under N_2 over Na immediately prior to use. Dimethylformamide, DMF, was treated with 4-Å molecular sieves after purchase from Baker Chemicals. When DMF was ob-

(20) Rhodes, R. K.; Kadish, K. M. *Anal. Chem.* **1981**, *53*, 1539–1541.
(21) Leggett, D. J.; McBryde, W. A. *Anal. Chem.* **1975**, *47*, 1065–1070.
(22) Leggett, D. J. *Anal. Chem.* **1977**, *49*, 276–281.
(23) Leggett, D. J.; Kelly, S. L.; Shiue, L. R.; Wu, Y. T.; Chang, D.; Kadish, K. M. *Talanta* **1983**, *30*, 579–586.
(24) Adler, A. D.; Longo, F. R.; Finarelli, R. D.; Goldmacher, J.; Assour, J.; Korsakoff, L. *J. Org. Chem.* **1967**, *32*, 476.
(25) Barnett, G. H.; Hudson, M. F.; Smith, K. M. *Tetrahedron Lett.* **1973**, 2887.
(26) Landrum, J. T.; Hatano, K.; Scheidt, W. R.; Reed, C. A. *J. Am. Chem. Soc.* **1980**, *102*, 6720–6735.
(27) Reed, C. A.; Mashiko, T.; Bentley, S. P.; Kastner, M. E.; Scheidt, W. R.; Spartalian, K.; Lang, G. *J. Am. Chem. Soc.* **1979**, *101*, 2948–2958.
(28) Van Duyne, R. P.; Reilley, C. *Anal. Chem.* **1972**, *44*, 142–152.

tained from Eastman Chemical, it was first shaken with KOH, distilled from CaO under N_2, and stored over 4-Å molecular sieves before use. Pyridine, py, was distilled over KOH.

Results and Discussion

Redox Reactions of (TPP)CrCl and (TPP)CrClO$_4$ in MeCl$_2$ Solutions. Cyclic voltammograms of (TPP)CrCl and (TPP)CrClO$_4$ in MeCl$_2$/0.1 M TBAP solution are shown in Figure 1. At a Pt electrode, three reversible processes and one irreversible process are observed in the range from +1.5 to −1.5 V vs. SCE.

The first reductions of both (TPP)CrCl and (TPP)CrClO$_4$ are irreversible (slow) and are characterized by decreased current maxima and broadened peak shape. This reduction has been shown in a previous study on (TPP)CrCl[16] to involve reduction of the central metal with subsequent loss of counterion, according to reaction 1. One may assume that reaction

$$(TPP)CrX \xrightarrow{e^-,\ irrev} (TPP)Cr + X^- \qquad (1)$$

1 also occurs for (TPP)CrClO$_4$, and stabilization of Cr^{3+} by axially bound chloride makes the metal-centered reduction of (TPP)CrCl harder than that of (TPP)CrClO$_4$ by some 200 mV. (At a scan rate of 100 mV/s, $E_{p,c}$ = −1.01 V for (TPP)CrCl and $E_{p,c}$ = −0.81 V for (TPP)CrClO$_4$.)

The second reduction is reversible, with $E_{1/2}$ = −1.20 V for both complexes. This reaction has been identified in previous studies[2,16] as the first reduction of the porphyrin ring (reaction 2). The independence of reaction 2 upon counterion is further

$$(TPP)Cr \rightleftharpoons [(TPP)Cr]^- \qquad (2)$$

evidence that reaction 1 occurs with loss of counterion. A further reversible reduction has been observed at −1.86 V vs. SCE for (TPP)CrCl (not shown in Figure 1) and can be assigned to the second reduction of the porphyrin ring (reaction 3).

$$[(TPP)Cr]^- \rightleftharpoons [(TPP)Cr]^{2-} \qquad (3)$$

The first oxidation is reversible for both complexes but exhibits a counterion dependance in all solvents studied. In MeCl$_2$ solution, (TPP)CrCl is easier to oxidize ($E_{1/2}$ = +0.87 V) than (TPP)CrClO$_4$ ($E_{1/2}$ = +1.03 V) by some 160 mV. The counterion dependence for this reaction is similar to that observed for the metal-centered reduction of (TPP)MnX[29] but is significantly smaller than for the metal-centered reduction of (TPP)FeX.[30] Although recent ESR and spectroscopic investigations[31] of the one-electron oxidation product of (TPP)CrCl in MeCl$_2$ were inconclusive as to the site of electron transfer, the counterion dependence suggests metal-centered oxidation, which agrees with earlier electrochemical studies.[2] It is interesting to note that the second oxidation potential also shows a dependence upon counterion. Oxidation of the chloride complex ($E_{1/2}$ = +1.29 V) is again easier than for the perchlorate complex ($E_{1/2}$ = +1.39 V), although the observed difference in oxidation potentials has been reduced to 100 mV.

Studies of (TPP)CrClO$_4$ in Mixed-Solvent Systems. The conductometric and spectrophotometric studies of Basolo, Hoffman, and others[11] on the ligand-binding properties of (TPP)CrCl have shown that while (TPP)Cr(L)Cl forms readily for a number of axial ligands (reaction 4), the symmetric six-coordinate species $[(TPP)Cr(L)_2]^+$ does not form to any appreciable extent (reaction 5). As it is probable that reaction 5 occurs through initial dissociation of chloride from (TPP)Cr(L)Cl,[14] the strong affinity of Cr^{3+} for chloride may prevent formation of $[(TPP)Cr(L)_2]^+$. The cyclic voltammetric studies in MeCl$_2$ clearly show perchlorate to interact less strongly than chloride with Cr^{3+}, and one might anticipate that reaction 5 will occur for (TPP)CrClO$_4$.

$$(TPP)CrX + L \rightleftharpoons (TPP)Cr(L)X \qquad (4)$$

$$(TPP)Cr(L)X + L \rightleftharpoons [(TPP)Cr(L)_2]^+ + X^- \qquad (5)$$

Table I lists the absorbance maxima of (TPP)CrCl and (TPP)CrClO$_4$ in the bonding solvents DMF, Me$_2$SO, and pyridine containing 0.1 M TBAP. There is a counterion dependence observed in the absorbance maxima, especially for the visible bands. Since the chloride complex exists as (TPP)Cr(L)Cl in these solvents,[12,15] the spectral differences between the perchlorate and chloride complexes may be due to the presence of either (TPP)Cr(L)ClO$_4$ or $[(TPP)Cr(L)_2]^+$ in solution. The conductometric and spectrophotometric studies to be reported here suggest the latter species is the more likely possibility.

Table II lists the equivalent conductances for millimolar concentrations of (TPP)CrClO$_4$ and (TPP)CrCl in 11 nonaqueous, aprotic solvents. For comparison purposes, the equivalent conductance of 10^{-3} M TBAP is included, which is assumed to behave as a 1:1 electrolyte. Excepting THF and the chlorinated solvents MeCl$_2$ and EtCl$_2$, the equivalent conductances of (TPP)CrClO$_4$ are comparable to those of TBAP. This suggests that the perchlorate complex undergoes considerable dissociation in most solvents. In contrast, the equivalent conductances of (TPP)CrCl are much lower than expected for a 1:1 electrolyte. Even in strongly coordinating media, the values are initially low. As seen in Table II, coordinating solvents with a high dielectric constant (DMA, DMF, Me$_2$SO) show a significant increase in conductance after 1 week, while low dielectric constant solvents (THF, pyridine) show no significant change. If the conductance increase in these solvents can be attributed to reaction 5, then there could be a rate-determining step that is favored for solvents of high dielectric constant. The data suggest that the rate-determining step for reaction 5 is the dissociation of Cl from (TPP)CrCl, which would be favored in solvents of high dielectric constant.

Table II. Equivalent Conductances (Ω^{-1} cm^{-1} equiv) of 10^{-3} M TBAP, (TPP)CrClO$_4$, and (TPP)CrCl in Selected Solvents

solvent	TBAP	(TPP)-CrClO$_4$	(TPP)CrCl[a] 0.1 h	18 h	42 h	168 h
EtCl$_2$	44.7	19.1	1.2			
MeCl$_2$	48.6	22.8	1.6			
PhCN	87.0	79.9	3.9			
MeCN	323.2	375.3	14.7			
n-PrCN	169.8	223.1	9.2			
(CH$_3$)$_2$CO	300.2	363.2	19.9			
THF	8.7	41.1	2.3	1.9	1.9	2.8
DMF	203.3	188.3	21.1	26.7	31.5	51.0
DMA	144.5	152.1	14.1	14.0	14.9	43.7
Me$_2$SO	92.0	88.5	13.9	17.3	19.7	38.2
py	94.1	134.8	12.3	12.9	13.7	15.0

[a] The equivalent conductances of (TPP)CrCl were measured after time intervals to ascertain the presence or absence of slow counterion displacement.

Analysis of the spectral and electrochemical behavior of (TPP)CrClO$_4$ in mixed-solvent systems also suggests the formation of bisligated species in solution. Figure 2 shows the absorbance changes in the visible bands of 10^{-4} M (TPP)CrClO$_4$ in MeCl$_2$/0.1 M TBAP solution as pyridine is added to solution. Addition of pyridine causes bands III and IV to shift slightly to the red, and the relative intensities of the bands are reversed. Although there are apparently isosbestic points

(29) Kelly, S. L.; Kadish, K. M. *Inorg. Chem.* **1982**, *21*, 3631–3639.
(30) Bottomley, L. A.; Kadish, K. M. *Inorg. Chem.* **1981**, *20*, 1348–1357.
(31) Carnieri, N.; Harriman, A. *Inorg. Chim. Acta* **1982**, *62*, 103–107.

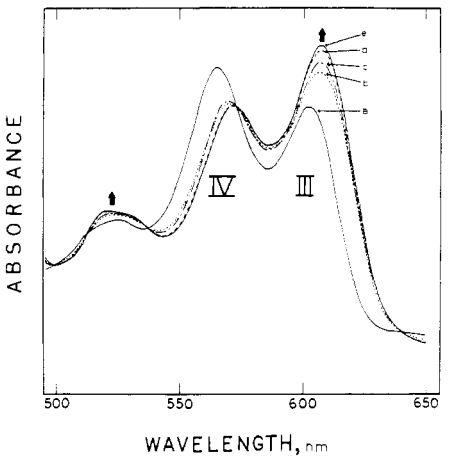

Figure 2. Absorbance changes observed in the visible spectra of 10^{-4} M (TPP)$CrClO_4$ dissolved in $MeCl_2$/0.1 M TBAP as pyridine is added to solution. Concentration of pyridine: (a) 0.00 M, (b) 8.91×10^{-5} M, (c) 1.78×10^{-4} M, (d) 3.55×10^{-4} M, (e) 1.02×10^{-2} M.

at 513, 537, 573, and 640 nm, there are spectral regions at low pyridine concentrations where the absorbance trends reverse themselves. This is most evident for band IV. Analysis of the absorbance data at 608 nm via the Benesi–Hildebrandt method[32-34] shows a slope of 2.0 ± 0.1, indicating the addition of two pyridine molecules to (TPP)$CrClO_4$, with the approximate overall formaton constant of log β_2^{III} = 8.0. However, contrary to the requirements of the B–H method,[35] similar slopes and intercepts were not obtained at other wavelengths. Analysis of the spectral data by SQUAD,[21-23] a sophisticated computer program that tests various equilibrium models to an absorbance data set, shows definitely that both the mono- and bis(pyridine) adducts form, with respective formation constants of log K_1^{III} = 4.2 ± 0.2 and log β_2^{III} = 8.1 ± 0.1. This value for log K_1^{III} compares favorably with that obtained spectrophotometrically for the displacement of acetone by pyridine to form (TPP)Cr(py)Cl (log K_{eq}^{III} = 4.3).[12]

Electrochemical measurements in $MeCl_2$/pyridine solvent mixtures corroborate formation of the bis(pyridine) adduct from (TPP)$CrClO_4$. The presence of 2–3 equiv of pyridine brings electrochemical reversibility to the metal-centered reduction, with $E_{1/2}$ = −0.77 V vs. SCE. The half-wave potential for this reaction is invariant with further addition of pyridine up to a concentration of 3.0 M. It is interesting to note that in a similar solvent mixture, the metal-centered reduction of (TPP)CrCl has been determined to occur by the two possible mechanisms shown in reactions 6 and 7.[15] As only (TPP)-

$$(TPP)Cr(py)Cl \overset{e^-}{\rightleftharpoons} [(TPP)Cr(py)Cl]^- \qquad E_p = -1.07 \text{ V} \tag{6}$$

$$[(TPP)Cr(py)_2]^+ \overset{e^-}{\rightleftharpoons} (TPP)Cr(py)_2 \qquad E_p = -0.75 \text{ V} \tag{7}$$

Cr(py)Cl exists in the bulk of solution, reaction 6 is the only reaction during the initial potential scan. Repeated potential cycling creates $[(TPP)Cr(py)_2]^+$ at the electrode surface, so that subsequent potential scans reveal the presence of reaction 7. The potentials of reactions 6 and 7 were determined by cyclic differential-pulse voltammetry[15] to be approximately −1.07 and −0.75 V vs. SCE, respectively. The similarity in potentials for the metal-centered reduction of (TPP)$CrClO_4$ in $MeCl_2$/pyridine mixtures and that for reaction 7 in $EtCl_2$/pyridine mixtures implies equivalent reactions and thus the presence of $[(TPP)Cr(py)_2]^+$ in the bulk of solution for the perchlorate complex.

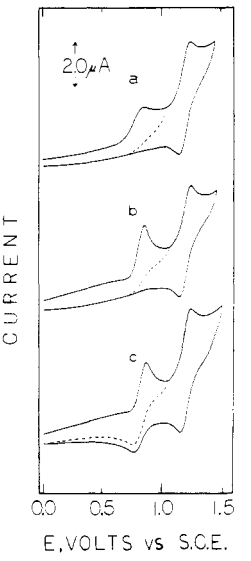

Figure 3. Cyclic voltammograms obtained during the titration of a 1 mM solution of (TPP)$CrClO_4$ dissolved in $MeCl_2$/0.1 M TBAP solution with Me_2SO (scan rate 0.20 V/s). Bulk concentration of Me_2SO: (a) 0.0 mM, (b) 2.0 mM, (c) 71.0 mM.

The less strongly coordinating solvent Me_2SO also seems able to displace perchlorate and form the bis(dimethyl sulfoxide) complex. Spectrophotometric studies show that addition of near stoichiometric amounts of Me_2SO causes an increase in the absorbance of the visible bands. Further addition of Me_2SO causes a gradual spectral change, with isobestic points maintained at 538, 566, and 603 nm. Analysis of the spectral data set by SQUAD shows the initial spectral change to correspond to the formation of (TPP)$Cr(Me_2SO)ClO_4$ (reaction 4), while the more gradual change (with the associated isobestic points) corresponds to the formation of $[(TPP)Cr(Me_2SO)_2]^+$ (reaction 5). Estimates of the formation constant are log K_1^{III} = 3.8 ± 0.1 and log β_2^{III} = 7.4 ± 0.1.

Electrochemical studies of (TPP)$CrClO_4$ in $MeCl_2/Me_2SO$ mixtures confirm the formation of $[(TPP)Cr(Me_2SO)_2]^+$ and also highlight the possible pathways for the metal-centered reduction. As seen in Figure 3, addition of a 2:1 excess amount of Me_2SO changes the nature of electron transfer for this reduction more than it affects the reduction potential. The wave shape changes from a broad wave ($E_p - E_{p/2}$ = 90 mV) with a poorly defined peak (Figure 3a) to a sharp wave ($E_p - E_{p/2}$ = 50 mV) with a well-defined peak (Figure 3b). This change in wave shape is assumed to be associated with the formation of (TPP)$Cr(Me_2SO)ClO_4$. This assumption follows from the fact that a similar complex, (TPP)Cr(L)Cl, has been shown to form readily in solution for ligands as weakly coordinating as acetone.[11,12] Although there is not an oxidation wave coupled to the reduction at this concentration, values of $i_{p,c}/v^{1/2}$ are constant, indicating diffusion control. At this ligand concentration, however, the current–potential curves as a function of scan rate are consistent with a rapid chemical reaction following electron transfer (EC mechanism). The Cr(III)/Cr(II) couple gains reversibility at Me_2SO concentrations above 0.07 M (Figure 3c), and, as shown in Figure 4a, the half-wave potential then depends upon the concentration of ligand. Initially there is a negative shift of 110 mV per decadic increase in Me_2SO concentration, indicating loss of two ligands upon reduction of Cr(III). Above 0.3 M Me_2SO, both the Cr(III) reduction and the first-ring reduction

(32) Hill, A. V. *J. Physiol. (London)* **1910**, *IVP*, *40*, iv–vii.
(33) Bent, J. C.; French, C. L. *J. Am. Chem. Soc.* **1941**, *63*, 548.
(34) Benesi, H. A.; Hildebrandt, J. H. *J. Am. Chem. Soc.* **1949**, *71*, 2703–2727.
(35) Rosotti, F. J. C.; Rosotti, H. S. In "The Determination of Stability Constants"; McGraw-Hill: New York, 1961.

Table III. Half-Wave Potentials (V) for the Electrode Reactions of (TPP)CrClO$_4$ in Selected Solvents

		oxidn				redn						
		$E_{1/2}^{(2)}$		$E_{1/2}^{(1)}$		$E_{1/2}^{(1)}$		$E_{1/2}^{(2)}$		$E_{1/2}^{(3)}$		$E_{1/2}^{-}$
no.	solvent	vs. SCE	vs. Fc/Fc$^+$	vs. SCE	vs. Fc/Fc$^+$	vs. SCE	vs. Fc/Fc$^+$	vs. SCE	vs. Fc/Fc$^+$	vs. SCE	vs. Fc/Fc$^+$	(Fc/Fc$^+$)
1	$MeCl_2$	+1.39	+0.90	+1.03	+0.54	(−0.81)[a]	(−1.30)[a]	−1.19	−1.68			+0.49
2	$EtCl_2$	+1.41	+0.90	+1.06	+0.55	(−0.81)[a]	(−1.32)[a]	−1.17	−1.68			+0.51
3	PhCN			+1.12	+0.65	−0.80	−1.26	−1.16	−1.63	−1.80	−2.26	+0.46
4	MeCN	+1.42	+1.02	+1.08	+0.68	−0.73	−1.13	−1.14	−1.54	−1.78	−2.18	+0.41
5	*n*-PrCN	+1.46	+0.97	+1.15	+0.66	−0.71	−1.19	−1.10	−1.58	−1.80	−2.28	+0.49
6	$(CH_3)_2CO$	+1.45	+0.96	+1.14	+0.65	(−0.79)[a]	(−1.27)[a]	−1.09	−1.56	−1.78	−2.26	+0.48
7	THF					−0.64	−1.21	−1.18	−1.74	−1.79	−2.36	+0.56
8	DMF			+1.14	+0.65	−0.85	−1.34	−1.12	−1.60	−1.72	−2.22	+0.49
9	DMA			+1.12	+0.61	−0.84	−1.35	−1.10	−1.60	−1.75	−2.25	+0.50
10	Me_2SO					−0.88	−1.34	−1.25	−1.71	−1.69	−2.15	+0.46
11	py					−0.65	−1.17	−1.42	−1.94			+0.52

[a] Potentials are quoted for $E_{p,c}$ at a scan rate of 100 mV/s. No anodic wave was observed in these solvents.

Scheme I

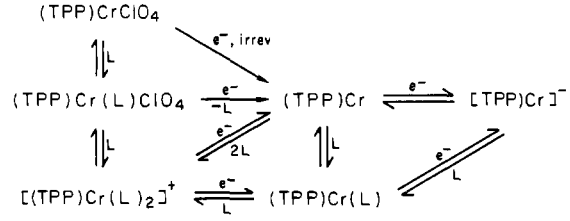

of Cr(II) shift negatively by 60 ± 5 mV per decadic increase in ligand concentration. This potential dependence is consistent with the reactions shown in Scheme I.

The metal-centered reduction for (TPP)CrClO$_4$ can be described as kinetically slow and irreversible. Addition of small concentrations of ligand allows formation of (TPP)Cr(Me$_2$SO)X, whose reduction is diffusion controlled but involves a rapid chemical reaction after electron transfer; thus, no oxidation current is observed for this reaction. Ligand concentrations above 0.1 M favor formation of [(TPP)Cr(Me$_2$SO)$_2$]$^+$, for which the metal-centered reduction is both diffusion controlled and reversible. Over a small concentration range this reduction exhibits a negative shift in $E_{1/2}$ of 110 mV, showing the reduced species to be (TPP)Cr. Above 0.3 M ligand the reduced product is (TPP)Cr(Me$_2$SO), as evidenced by the observed negative shift of 60 ± 5 mV for both the metal-centered and ring-centered reductions. The formation constant for the addition of Me$_2$SO to (TPP)Cr^{II} was determined to be log K_1^{II} = 0.8 via application of the modified Nernst equation to the potential shifts for the first-ring reduction.

As seen in Figure 4b, electrochemical measurements in MeCl$_2$/DMF mixtures also give evidence for bis coordination by [(TPP)Cr]$^+$. Addition of stoichiometric amounts of DMF again change the metal-centered reduction wave from a broad shape characteristic of irreversible electron transfer to a sharp, well-defined shape characteristic of a diffusion-controlled electron transfer followed by a rapid chemical reaction. However, reversibility for this reaction is not attained until DMF concentrations are above 0.25 M. The negative shift of the reversible reduction ($\Delta E_{1/2}/\Delta$(log [DMF]) = −120 mV) again indicates that the reversibility is associated with formation of [(TPP)Cr(DMF)$_2$]$^+$ in the bulk of solution, which reduces according to reaction 8. Over the range of DMF

$$[(TPP)Cr(DMF)_2]^+ \overset{e^-}{\rightleftharpoons} (TPP)Cr + 2DMF \qquad (8)$$

concentrations studied, the first-ring reduction remains independent of DMF concentration. Thus, there is no electrochemical evidence for DMF binding to the reduced species, as was the case for Me$_2$SO. This can be attributed to the weaker coordinating ability of DMF relative to Me$_2$SO.

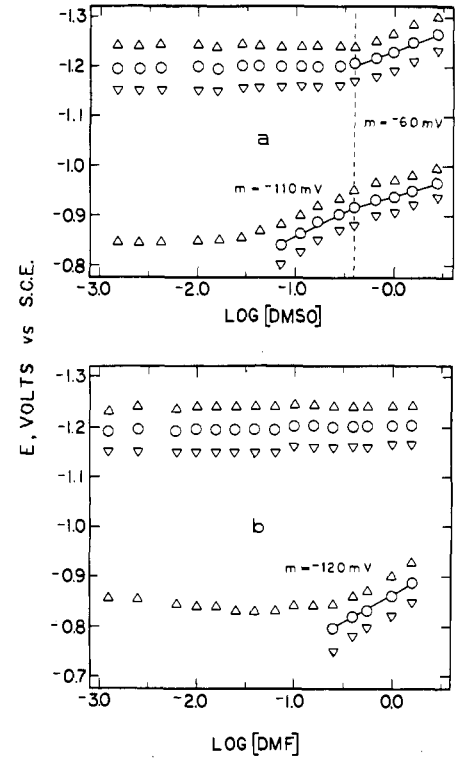

Figure 4. Plots of $E_{p,c}$ (Δ), $E_{p,a}$ (∇), and $E_{1/2}$ (O) vs. logarithmic ligand concentration for the first two reductions of 10^{-3} M (TPP)CrClO$_4$ dissolved in MeCl$_2$/0.1 M TBAP solution where (a) L = Me$_2$SO and (b) L = DMF.

However, the mixed-solvent studies seem to establish a strong link between absence of axially coordinated counterion and reversibility for the metal-centered reduction.

Solvent and Counterion Effects on the Metal-Centered Reduction of (TPP)CrX. Table III lists potentials for the various redox reactions of (TPP)CrClO$_4$ in the 11 solvents studied. It is interesting to compare the effect of solvent and counterion on the metal-centered reduction of (TPP)CrX, where X = Cl$^-$ and ClO$_4^-$. The recent work on Bottomley et al.[16] showed that the metal-centered reduction of (TPP)CrCl is irreversible in all solvents except DMA, DMF, Me$_2$SO, and pyridine. In contrast, the metal-centered reduction of (TPP)CrClO$_4$ is reversible in all solvents except MeCl$_2$, EtCl$_2$, and acetone. Inspection of the conductivity data in Table II shows, with the exception of acetone, a good correlation exists between the extent of (TPP)CrClO$_4$ dissociation and the reversibility of the Cr(III) ⇄ Cr(II) reaction. This further reinforces the conclusion obtained from mixed-solvent studies that the necessary requirement for electrochemical reversibility is the absence of an axially coordinated counterion. However, the

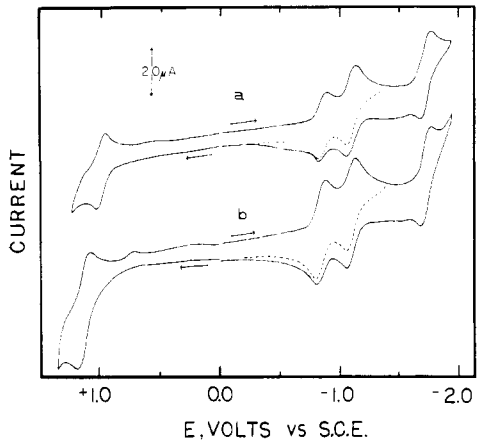

Figure 5. Cyclic voltammograms of (a) 10^{-3} M (TPP)$CrClO_4$ and (b) 1.5×10^{-3} M (TPP)CrCl dissolved in DMF/0.1 M TBAP solutions (scan rate 0.20 V/s).

conductance data for (TPP)CrCl does not support this conclusion, as a reversible metal-centered reduction for this compound occurs in DMA, DMF, and Me_2SO, in spite of the low conductances of these solutions.

The nature of the problem is highlighted in Figure 5, which shows cyclic voltammograms for millimolar concentrations of (TPP)$CrClO_4$ and (TPP)CrCl in DMF/0.1 M TBAP solution. The conductivity measurements shown in Table II as well as the mixed-solvent studies suggest that the perchlorate complex exists as $[(TPP)Cr(DMF)_2]^+$ in DMF solution, while the chloride complex exists as (TPP)Cr(DMF)Cl. The results for the first oxidation agree with the conclusion that different species are present in solution, as there is a 140-mV difference in half-wave potential between oxidation of the perchlorate ($E_{1/2}$ = +1.14 V) and chloride ($E_{1/2}$ = +1.00 V) complexes. However, the half-wave potentials measured for the first reduction are independent of counterion ($E_{1/2}$ = −0.86 V for both complexes). If one assumes that there are no chemical reactions that precede or follow this reduction, one must also assume either that both $[(TPP)Cr(DMF)_2]^+$ and (TPP)Cr(DMF)Cl reduce at identical potentials or that identical species exist in solution. This latter assumption contradicts the counterion dependence found for the first oxidation as well as conductometric measurements. Thus, the best explanation for these identical reduction potentials is that dissociation of chloride from TPP(DMF)Cl occurs at the electrode surface before reduction, with the applied potential acting as the driving force for this dissociation. A similar mechanism was found to apply for the reduction of (TPP)CrCl in pyridine solutions.[15,16] This explanation supports the conclusion that a necessary criterion for the electrochemically reversible metal-centered reduction of chromium porphyrins is the absence of an axially coordinated counterion.

Redox Reactions of (TPP)Cr(NO) in $MeCl_2$ Solutions. (TPP)Cr(NO) exhibits one irreversible and four reversible redox processes at a Pt electrode in the range +1.6 to −2.0 V vs. SCE. As seen in Figure 6b, both reductions of (TPP)Cr(NO) are reversible processes and may be written

$$(TPP)Cr(NO) \overset{e^-}{\rightleftharpoons} [(TPP)Cr(NO)]^- \quad (9)$$

$$[(TPP)Cr(NO)]^- \overset{e^-}{\rightleftharpoons} [(TPP)Cr(NO)]^{2-} \quad (10)$$

The potential separation between the two reactions is consistent with that reported for most metalloporphyrin ring-centered reductions (420 ± 50 mV).[36] Also, the first reduction of (TPP)Cr(NO) ($E_{1/2}$ = −1.24 V) corresponds fairly closely in potential to that for the first-ring reduction of (TPP)CrX in the same solvent.

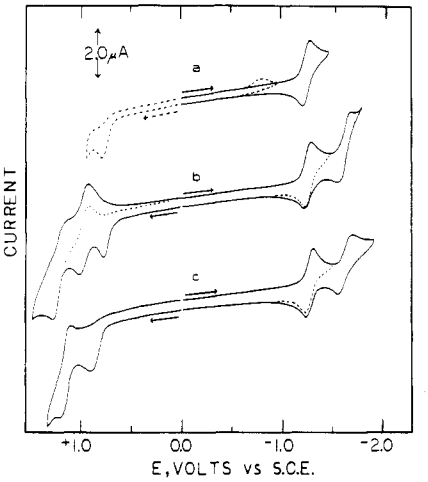

Figure 6. Cyclic voltammograms of (a) 10^{-3} M (TPP)Cr(NO) dissolved in $MeCl_2$/0.1 M TBAP solution, (b) the same solution as in (a) but with a broader potential scan range, and (c) 10^{-3} M (TPP)Cr(NO) dissolved in DMF/0.1 M TBAP solution.

The first oxidation of (TPP)Cr(NO) is irreversible in all solvents studied, with $E_{p,a}$ = +0.79 V vs. SCE at a scan rate of 200 mV/s in $MeCl_2$/0.1 M TBAP solution. As seen in Figure 6b, the second and third oxidations are reversible, with $E_{1/2}$ = +0.95 and +1.22 V vs. SCE, respectively. The potentials for the latter two reactions are comparable to the first two oxidations of (TPP)$CrClO_4$ and of (TPP)CrCl. If the first oxidation of (TPP)Cr(NO) involved chemical reaction or loss of bound NO after electron transfer, then it would be expected that (TPP)Cr(NO) and (TPP)$CrClO_4$ would have similar potentials for any further oxidation reactions. We suggest that this indeed does occur and that the second oxidation of (TPP)Cr(NO) and the first oxidation of (TPP)CrX correspond to an electrode reaction of similar species. In this case, the reacting species would be (TPP)$CrClO_4$ (or $[(TPP)Cr]^+$), which is generated at the electrode surface after a reversible (rapid) oxidation of (TPP)Cr(NO) according to eq 11.

$$(TPP)Cr(NO) \xrightarrow{-e^-} [(TPP)Cr(NO)]^+ \rightarrow [(TPP)Cr]^+ + NO \quad (11)$$

Proof of the EC mechanism shown in eq 11 comes from the current–voltage curves for oxidation of (TPP)Cr(NO) as well as from spectral monitoring of the first oxidation products. The first oxidation of (TPP)Cr(NO) has a peak geometry ($E_p - E_{p/2} = 60 \pm 10$ mV) consistent with a reversible, one-electron transfer followed by a rapid chemical reaction.[37] This well-shaped oxidation peak (E_p = +0.79 V with a scan rate of 0.1 V/s) is not reversibly coupled to a reduction process near this potential but, rather, generates a new peak at −0.82 V, which does not have a reverse peak. This peak at negative potentials (shown in Figure 6a) is not present until the potential is scanned to values more positive than +0.80 V. It can be seen in Figure 1b that a similar irreversible reduction process is observed at −0.81 V for (TPP)$CrClO_4$ in $MeCl_2$ (reaction 1) and strongly suggests that (TPP)$CrClO_4$ is generated after oxidation of (TPP)Cr(NO), as shown in reaction 11. The reduced current for the reduction process at −0.81 V, when compared to the oxidation process at +0.79 V, is not unexpected and is consistent with an irreversible reduction process whose current depends upon the transfer coefficient α.[37]

Further corroboration of the above suggested mechanism is found in the electronic absorption spectra. The one-electron

(36) Fuhrhop, J.-H.; Kadish, K. M.; Davis, D. G. *J. Am. Chem. Soc.* **1973**, *95*, 5140–5147.

(37) Nicholson, R. S.; Shain, I. *Anal. Chem.* **1964**, *36*, 706–723.

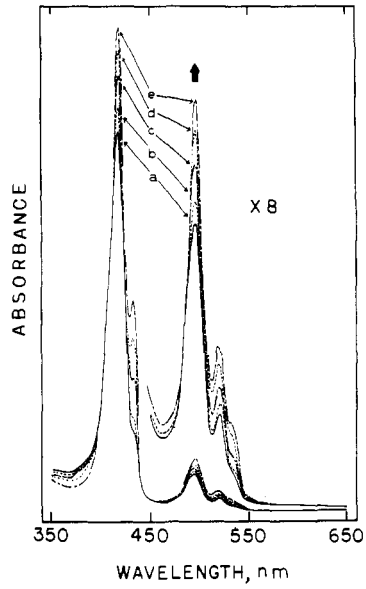

Figure 7. Absorbance changes observed for 10^{-4} M (TPP)Cr(NO) dissolved in $MeCl_2$/0.1 M TBAP solution as DMF is added to solution. Concentration of DMF: (a) 0.00 M, (b) 2.57×10^{-5} M, (c) 1.55×10^{-4} M, (d) 6.17×10^{-4} M, (e) 4.47×10^{-3} M.

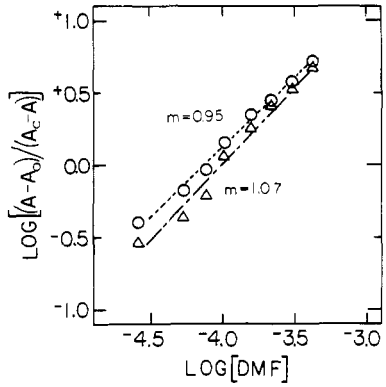

Figure 8. Benesi–Hildebrandt plot of absorbance data shown in Figure 7. Wavelengths analyzed are 425 nm (○) and 498 nm (△).

oxidation product of (TPP)Cr(NO) generated by bulk electrolysis is spectrally similar to that of (TPP)CrX.[11] The oxidized solution showed no sign of a reverse cathodic current until potentials more negative than −0.8 V vs. SCE were applied. Also, the return one-electron reduction of the oxidized species did not exhibit the UV–visible spectra of (TPP)Cr(NO),[10] but rather that of (TPP)Cr.[17] Experiments using an optically transparent thin-layer electrode (OTTLE) resulted in the same spectral behavior as seen by bulk electrolysis experiments. It is interesting to note that no evidence for the presence of NO in solution was found after the metal-centered oxidation had occurred.

Studies of (TPP)Cr(NO) in Mixed-Solvent Systems. The reactions of (TPP)Cr(NO) were investigated in mixed-solvent systems containing $MeCl_2$ and either DMF, Me_2SO, or pyridine. In all cases the solvent acted as an axial ligand, as shown in reaction 12. This is shown in Figure 7, which illustrates

$$(TPP)Cr(NO) + L \rightleftharpoons (TPP)Cr(NO)(L) \qquad (12)$$

the spectral changes that occur upon going from $MeCl_2$ to $MeCl_2$/DMF mixtures as a solvent. As seen in this figure, the main spectral change upon addition of DMF to (TPP)Cr(NO) in $MeCl_2$ is an increase in the absorbances of all peaks. A new absorption at 445 nm also appears and can be attributed to the formation of some $[(TPP)Cr(DMF)_2]^+$ (or (TPP)Cr(DMF)X) at high DMF concentrations. DMF did not cause displacement of NO until its mole ratio was quite high. A similar result was observed with Me_2SO as a ligand, while pyridine produced a mixture of (TPP)Cr(NO)(py) and $[(TPP)Cr(py)_2]^+$ at levels exceeding 1 M py in $MeCl_2$. Analysis of the absorbance changes at 425 and 498 nm via the Benesi–Hildebrandt method[32-34] yielded slopes of 1.0 ± 0.1 (Figure 8), which indicates that only one ligand is involved in complex formation.

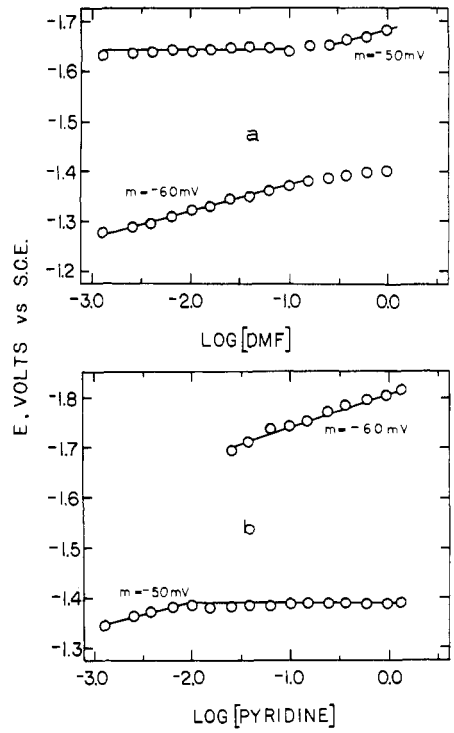

Figure 9. Plots of $E_{1/2}$ vs. logarithmic ligand concentration for the first two reductions of 10^{-3} M (TPP)Cr(NO) dissolved in $MeCl_2$/0.1 M TBAP solution where (a) L = DMF and (b) L = pyridine.

Scheme II

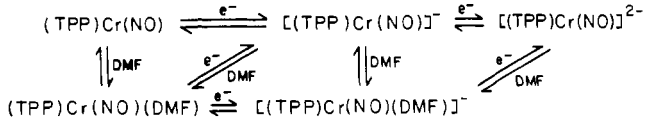

Calculations of log K for reaction 12 gave values of 4.1 ± 0.2 for L = DMF. On the basis of this formation constant, one can calculate that DMF will bind to (TPP)Cr(NO) at low DMF concentrations and that a cathodic shift of potential will be observed for the first reduction of (TPP)Cr(NO)(DMF) if the reduced product is not also strongly complexed by a DMF molecule. This, indeed, is the case, as shown in Figure 9a, which plots $E_{1/2}$ for the first two reductions of (TPP)Cr(NO) in $MeCl_2$/DMF mixtures vs. the logarithmic concentration of DMF. The behavior of the reduction reactions can be divided into two concentration regions. In the lower concentration region ([DMF] < 0.3 M), a 60-mV negative shift in the first reduction potential per decadic increase in DMF concentration occurs, while the second reduction potential is independent of DMF concentration. In the second region (>0.3 M DMF), the first reduction potential is constant, while the second reduction potential undergoes a negative shift of 50 mV per decadic increase in DMF concentration.

This behavior is the type that can be unambiguously explained by application of the modified Nernst equation[38] and may be described by the sequence of reactions shown in Scheme II. At concentrations of DMF between 10^{-3} and 0.3

(38) Laitenen, H. A.; Harrison, W. E. "Chemical Analysis"; McGraw-Hill: New York, 1975; pp 227–231.

Table IV. Formation Constants for the Axial Ligation (L) of (TPP)$CrClO_4$ and (TPP)Cr(NO) by DMF, Me_2SO, and Pyridine

species	DMF	Me_2SO	pyridine
(TPP)Cr(L)Cl			4.3[b]
(TPP)Cr(L)ClO_4		3.8 ± 0.1	4.2 ± 0.2
$[(TPP)Cr(L)_2]^+$		7.4 ± 0.1	8.1 ± 0.1
(TPP)Cr(NO)(L)	3.1 (4.1)[a]	3.3 (3.7)[a]	4.2
$[(TPP)Cr(NO)(L)]^-$	0.6	1.0	2.1

[a] Estimates in parentheses determined from spectrophotometric data via the Hill equation. [b] Estimate obtained from ref 12 for the reaction (TPP)CrCl(S) + py ⇄ (TPP)CrCl(L) + S where S = acetone.

M a solvent molecule binds to (TPP)Cr(NO), but not to either of the reduced products. Thus, there is a change in coordination number during the first reduction and the potential of this reaction depends upon DMF concentration. The theoretical potential shift is 60 mV/log [DMF],[38] and this is what is experimentally observed. At concentrations of DMF above 0.3 M, binding to $[(TPP)Cr(NO)]^-$ by DMF also occurs, and the reduced product is $[(TPP)Cr(NO)(DMF)]^-$. For this case the theoretical shift of $\Delta E_{1/2}/\Delta(\log [DMF])$ for the first reduction is zero,[38] and this is approached experimentally (greater than 1.0 M DMF concentrations are actually needed to achieve this condition). At all ligand concentrations, the second reduction causes loss of DMF. Thus, above 0.3 M DMF, the half-wave potential for the second reduction shifts cathodically by 60 mV per decade, which confirms the formation of $[(TPP)Cr(NO)(DMF)]^-$ under these conditions.

Finally, stability constants were calculated for addition of DMF to (TPP)Cr(NO) (reaction 12) and $[(TPP)Cr(NO)]^-$ (reaction 13) with use of the measured shifts in half-wave

$$[(TPP)Cr(NO)]^- + L \rightleftharpoons [(TPP)Cr(NO)(L)]^- \quad (13)$$

potentials as a function of DMF concentration. These values are log K = 3.11 and 0.66 and are listed in Table IV. The former value is almost 1 full order of magnitude lower than that measured by spectrophotometric techniques. No explanation for this deviation is evident, other than that different concentrations of metalloporphyrin are used for the two titration experiments.

The electrochemical and spectral behavior of (TPP)Cr(NO) in $Me_2SO/MeCl_2$ and $py/MeCl_2$ mixtures was characterized and was very similar to that observed in $DMF/MeCl_2$ solutions. In all three solvent mixtures both (TPP)Cr(NO) and $[(TPP)Cr(NO)]^-$ could be axially complexed by solvent, and a negative potential shift was observed. This is shown in Figure 9b where L = py. The form of the plot is similar to that shown in Figure 9a, and the mechanism is identical with that in Scheme II. Pyridine is a stronger ligand than DMF and, as such, complexes to (TPP)Cr(NO) and $[(TPP)Cr(NO)]^-$ at much lower concentrations. Thus, the concentration of pyridine needed to induce a negative shift in the second reduction of (TPP)Cr(NO) is only 10^{-2} M. The well-developed relationship between $E_{1/2}$ and log [L] allows calculation of stability constants for the addition of pyridine to (TPP)Cr(NO) (reaction 12) and to $[(TPP)Cr(NO)]^-$ (reaction 13). A summary of stability constants for L = DMF, Me_2SO, and pyridine is presented in Table IV. It can be seen that the complex stability increases with increasing coordinating ability of the ligand for both oxidation states. Also, the formation constants for the addition of one pyridine to (TPP)Cr(NO) is comparable to those for the addition of one pyridine to (TPP)$CrClO_4$ and (TPP)CrCl.

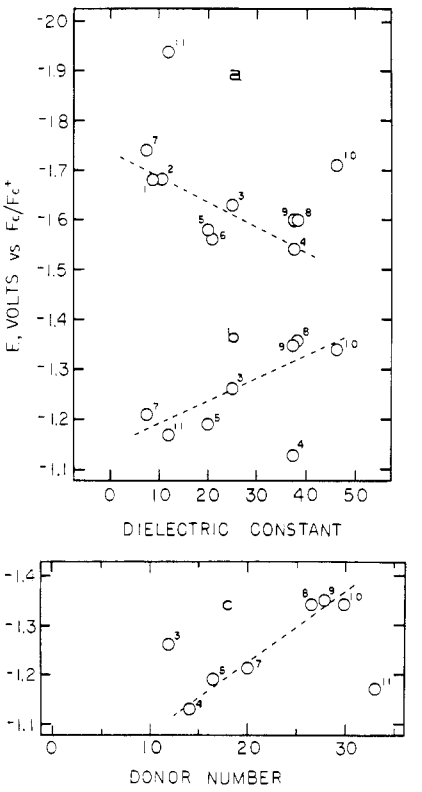

Figure 10. Plots of (a) $E_{1/2}$ vs. dielectric constant of the solvent for the reversible ring reduction of (TPP)$CrClO_4$, (b) $E_{1/2}$ vs. dielectric constant of the solvent for the reversible metal-centered reduction of (TPP)$CrClO_4$, and (c) $E_{1/2}$ vs. donor number of the solvent for the metal-centered reduction of (TPP)$CrClO_4$. Solvent numbers are given in Table III.

Solvent Effects on the Electrode Reactions of (TPP)$CrClO_4$ and (TPP)Cr(NO). Tables III and V list potentials of the various reactions of (TPP)$CrClO_4$ and (TPP)Cr(NO), respectively, in the solvents studied. By correlating the corrected potentials to a solvent parameter, one may hope to determine

Table V. Half-Wave Potentials (V) for the Electrode Reactions of (TPP)Cr(NO) in Selected Solvents[a]

		oxidn						redn				
		$E_{1/2}^{(3)}$		$E_{1/2}^{(2)}$		$E_p^{(1)a}$		$E_{1/2}^{(1)}$		$E_{1/2}^{(2)}$		$E_{1/2}$-
no.	solvent	vs. SCE	vs. Fc/Fc$^+$	vs. SCE	vs. Fc/Fc$^+$	vs. SCE	vs. Fc/Fc$^+$	vs. SCE	vs. Fc/Fc$^+$	vs. SCE	vs. Fc/Fc$^+$	(Fc/Fc$^+$)
1	$MeCl_2$	+1.22	+0.73	+0.95	+0.46	+0.79	+0.31	−1.24	−1.72	−1.63	−2.11	+0.48
2	$EtCl_2$			+1.11	+0.60	+0.79	+0.29	−1.27	−1.78	−1.58	−2.08	+0.50
3	PhCN			+1.18	+0.71	+0.86	+0.39	−1.27	−1.74			+0.47
4	MeCN					+0.54	+0.14	−1.30	−1.69			+0.40
5	*n*-PrCN	+1.43	+0.97	+1.14	+0.69	+0.84	+0.39	−1.30	−1.75	−1.64	−2.09	+0.45
6	$(CH_3)_2CO$			+1.16	+0.67	+0.84	+0.36	−1.27	−1.76	−1.62	−2.10	+0.48
7	THF							−1.32	−1.88	−1.66	−2.22	+0.56
8	DMF			+1.15	+0.66	+0.88	+0.39	−1.28	−1.77	−1.62	−2.11	+0.49
9	DMA			+1.22	+0.69	+0.85	+0.32	−1.28	−1.81	−1.61	−2.13	+0.53
10	Me_2SO					+0.91	+0.45	−1.27	−1.72	−1.61	−2.07	+0.46
11	py					+0.92	+0.40	−1.30	−1.82	−1.80	−2.33	+0.52

[a] Potentials are quoted for $E_{p,a}$ at a scan rate of 100 mV/s. See text for discussion.

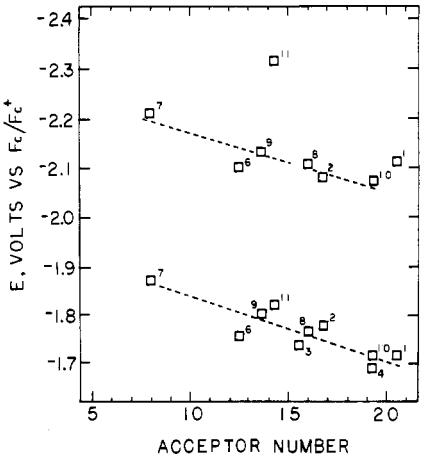

Figure 11. Plot of $E_{1/2}$ vs. acceptor number of the solvent for the first two reductions of (TPP)Cr(NO). Solvent numbers are given in Table V.

what solute–solvent interactions predominate for a given redox couple. The first-ring reduction of (TPP)CrClO$_4$ correlates best to the dielectric constant of the solvent (Figure 10a), except for the bonding solvents Me_2SO (10) and pyridine (11). The mixed-solvent studies discussed previously have highlighted how coordination greatly affects the potentials of the reduction reactions, so it is not surprising that these strongly coordinating solvents do not show the same behavior as noncoordinating and weakly coordinating solvents. Except for the solvents Me_2SO and pyridine, a stabilization of the reduced species over the oxidized species is observed with increasing dielectric constant. This behavior suggests that the much weaker dielectric interactions predominate for these solvents in the absence of strong coordinating effects. The fact that the reduced species is stabilized with increasing dielectric constant implies the importance of porphyrin-ring π electrons in these interactions.[39]

The potential dependence for the metal-centered reductions of (TPP)CrClO$_4$ is more difficult to explain. Figure 10b shows that this redox reaction correlates reasonably well (r = 0.92) to the solvent dielectric constant, excepting MeCN (4). However, excepting the solvents PhCN (3) and pyridine (11), a better correlation is found with solvent donor number (r = 0.99), as shown in Figure 10c. The stabilization of Cr^{3+} over Cr^{2+} with increasing donor number would be consistent with strong axial interactions between solvent and Cr^{3+} but relatively weak axial interactions between solvent and Cr^{2+}. The mixed-solvent studies reported here show this is indeed the case for the solvents DMF and Me_2SO. However, pyridine has been shown to interact strongly with Cr^{2+} (log β_2^{II} = 5.0 for the addition of two pyridines to (TPP)Cr^{2+}[16]); thus, one would expect a more positive $E_{1/2}$ in this solvent than found for other coordinating solvents.

In contrast to the reversible reductions of (TPP)CrClO$_4$, the first and second reversible reductions of (TPP)Cr(NO) correlate best to the acceptor number of the solvent (see Figure 11). Also, the potentials in bonding solvents show little deviation from the general trend. It seems that the ability of the solvent to accept the increased electron density of the reduced species is the primary factor in these reactions. The only exception from this behavior is seen for the second reduction of (TPP)Cr(NO) in pyridine (11), which can be explained by the unusually strong coordination of this solvent to [(TPP)Cr(NO)]$^-$, as discussed for the mixed-solvent studies (see Figure 9b). This strong bonding to [(TPP)Cr(NO)]$^-$ also explains why the potential separation between the two reductions of (TPP)Cr(NO) in pyridine are larger than normally expected for ring reductions.[36]

Summary. In conclusion, this work provides an in-depth study of the electron-transfer and ligand-addition reactions for the chromium porphyrins (TPP)CrClO$_4$ and (TPP)Cr(NO) in nonaqueous solvents. Specifically for (TPP)CrClO$_4$, this work provides the first clear evidence for the presence of symmetric, biscoordinated Cr^{3+} porphyrin complexes in solution. Spectrophotometric and electrochemical studies in mixed-solvent systems have provided stepwise formation constants for the addition of Me_2SO and pyridine to (TPP)CrClO$_4$ and have demonstrated how the axial environment about the central metal determines the electrochemical reversibility for the metal-centered reduction. Also, this work provides the first report on the electron-transfer and ligand-addition reactions for a diatomic molecule adduct of a chromium porphyrin, (TPP)Cr(NO). The studies have shown that nitrosylation stabilizes the divalent state of Cr by over 1.0 V and that metal-centered oxidation occurs via an EC mechanism. Determinations of formation constants for the addition of a ligand to (TPP)Cr(NO) have shown them to be comparable for the addition of a ligand to (TPP)CrX. Finally, analysis of the solvent effects on the redox reactions of (TPP)CrClO$_4$ and (TPP)Cr(NO) shows that the solvent–solute interactions that determine the relative stabilities for the various oxidation states differ between the two complexes.

Acknowledgment. The authors gratefully acknowledge support of this research from the National Science Foundation (Grant CHE-8215507). We also thank Dr. Paul Minor for the synthesis of (TPP)CrClO$_4$. S.L.K. acknowledges a summer fellowship from the Analytical Division of the American Chemical Society.

Registry No. (TPP)CrClO$_4$, 88563-13-7; (TPP)Cr(NO), 58356-56-2; (TPP)Cr(NO)(DMF), 88563-14-8; [(TPP)Cr(NO)(DMF)]$^-$, 88563-15-9; (TPP)Cr(Me_2SO)ClO$_4$, 88563-16-0; [(TPP)Cr(Me_2SO)$_2$]$^+$, 88563-17-1; (TPP)Cr(NO)(Me_2SO), 88563-18-2; [(TPP)Cr(NO)(Me_2SO)]$^-$, 88563-19-3; (TPP)Cr(py)ClO$_4$, 88563-20-6; [(TPP)Cr(py)$_2$]$^+$, 83665-06-9; (TPP)Cr(NO)(py), 88563-21-7; [(TPP)Cr(NO)(py)]$^-$, 88563-22-8; (TPP)CrCl, 28110-70-5.

(39) Gouterman, M.; Hanson, L. K.; Khalil, G.-E.; Leenstra, W. R. *J. Chem. Phys.* **1975**, *62*, 2343–2353.